Journal of Power Sources 219 (2012) 1–8

Contents lists available at SciVerse ScienceDirect

Journal of Power Sources

journal homepage: www.elsevier.com/locate/jpowsour

Low-cost shape-control synthesis of porous carbon film on β″-alumina ceramics for Na-based battery application

Yingying Hu, Zhaoyin Wen*, Xiangwei Wu, Jun Jin

CAS Key Laboratory of Materials for Energy Conversion, Shanghai Institute of Ceramics, Chinese Academy of Sciences, 1295 DingXi Road, Shanghai 200050, PR China

HIGHLIGHTS

► Fabricating uniform porous carbon films with tunable structural parameters on the surface of β″-alumina ceramics.
► Effective connection between carbohydrate and PMMA through hydrogen bonds.
► Largely improving the wettability of the β″-alumina surface by molten sodium.
► Alleviating the polarization problem of the sodium/β″-alumina interface in Na-based batteries by the porous coating.

ARTICLE INFO

Article history:
Received 25 April 2012
Received in revised form
5 July 2012
Accepted 11 July 2012
Available online 20 July 2012

Keywords:
Carbon
Porous
Beta-alumina
Polarization
Na-based battery

ABSTRACT

Porous carbon films with tunable pore structure to modify the β″-alumina electrolyte surface are fabricated through a low-cost and direct wet chemistry method with glucose and poly(methylmethacrylate) (PMMA) as precursors. FTIR analysis confirms the effective connection between the carbohydrate and the pore-forming agent PMMA through hydrogen bonds. The experimental results indicate that the structural parameters of the porous carbon films, including mean pore size and film thickness, can be tuned simply by adjusting the amount of PMMA in the glucose/PMMA composite. This soft-template-assisted method could be readily extended to modify any other ceramic surfaces. The porous carbon films are demonstrated to greatly improve the wettability of the β″-alumina ceramics by molten sodium. Na/β″-alumina/Na cells are used to investigate the interfacial properties between sodium and the β″-alumina electrolyte. The results obtained at 350 °C reveal that the polarization behavior of the cell is alleviated by the porous coating. This work represents a successful method to coat ceramics with porous carbon and offers a promising solution to overcome the polarization problems of the sodium/β″-alumina interface in Na-based batteries.

1. Introduction

Over the past few decades, medium-temperature Na batteries such as Na–S and sodium–metal halide batteries, which were based on a sodium ion conductive solid electrolyte have attracted great interests in the fields of energy conversion and storage devices because of their high efficiency, low cost, eco-friendly process and high energy density [1–4]. As known, the sodium ion conductor β″-alumina (rhombohedral; R3m; $a_0 = 0.560$ nm, $c_0 = 3.395$ nm) is the most practical solid electrolyte for the Na-based battery [3–6]. Even though its incremental developments were achieved in large capacity energy storage systems, the future of such a battery for actual applications lies in the improvement of its electrochemical performances and reliability, which are greatly dependent on the polarization at the sodium/β″-alumina interface mainly caused by incomplete wetting of β″-alumina by sodium [3,5]. A number of experimental evidences strongly implied that calcium impurity in the electrolyte had a negative influence on the interface behavior, leading to incomplete wetting of sodium on the β″-alumina ceramics [7,8]. The impurity can migrate to the sodium/β″-alumina interface and might be oxidized to form a film, which hampers sodium ion transport, and leads to the serious polarization in the cell [8,9].

Modifying the β″-alumina electrolyte surface is considered as an effective way to improve its wettability of sodium. For this purpose, many metal and oxide materials were employed to coat on the surface to decrease the contact angle between liquid sodium and the β″-alumina surface [10–12]. For example, coating the ceramic surface with a layer of lead was proved to significantly improve the wettability of the surface for sodium [13]. It was proposed that the coatings provided an increased surface area to lessen the

* Corresponding author. Tel.: +86 21 52411704; fax: +86 21 52413903.
E-mail addresses: zywen@mail.sic.ac.cn, liangxiao@student.sic.ac.cn (Z. Wen).

0378-7753/$ – see front matter
http://dx.doi.org/10.1016/j.jpowsour.2012.07.025

interference of calcium oxide. For this reason, porous films, which are liable to have higher surface area and more stable structure, were found to be a more suitable candidate. Some porous metals have been used in sodium electrode construction [14,15]. However, it is a challenge to realize a close contact between the β″-alumina ceramic and the porous materials. Direct fabrication of a porous coating on the β″-alumina surface becomes an attractive technique, which ensures robust mechanical adhesion and electrical contact between coating layer and the electrolyte.

In general, carbon materials are more readily wetted by molten metal than ceramics and possess good ability to conduct electric charge [16]. Coating the β″-alumina electrolyte with porous carbon would be an effective manner to improve the wettability of sodium. In recent years, some synthetic methods have been successfully applied to prepare porous carbon, such as the hard-template route [17,18] and direct template carbonization process [19], both of which required complicated procedures to prepare a template. In addition, sol–gel processes, usually with environmental pollutants [20], and soft-template routes based on self-assembly between costly block copolymers and carbohydrates [21,22] have also been employed. However, porous carbon films on substrates were seldom studied [23].

In this work, uniform porous carbon films (PCFs) with controlled pore texture were fabricated immediately on β″-alumina ceramic surface through a self-assembly between the poly(methyl-methacrylate) (PMMA) and carbohydrates in N,N-dimethylformamide (DMF) solution. The introduction of the porous carbon coating would greatly improve the wettability of the solid electrolyte surface for sodium, guaranteeing the good contact of Na with β″-alumina ceramics and the fast charge transport at the interface. In addition, the interfacial properties and polarization behavior of the Na/β″-alumina/Na cells with and without the PCF coating were studied by measuring the cyclic voltammograms, electrochemical impedance spectroscopy, and polarization potentials. The results indicated that the β″-alumina electrolyte coated the PCF exhibited better interfacial and reduced polarization in comparison with the pristine one.

2. Experimental

2.1. Materials

All chemicals are of analytical-grade without further purification. Glucose and DMF were supplied by Sinopharm Chemical Reagent Co. Ltd (China), while PMMA (average particle size: 59.7 μm) was from Aladdin Reagent Co. Ltd (China). β″-alumina ceramic disks (Φ10 mm × 1.5 mm), from Shanghai Institute of Ceramics, Chinese Academy of Sciences [24], had a chemical composition of 9.0 wt% Na_2O + 0.72 wt% Li_2O, with the balance being alumina with a β″ content of >99% and the relative density >99%. The disks were pretreated by sonication in anhydrous ethanol and dried in air at 100 °C for 5 h, then stored in a drying cupboard for later use.

2.2. Preparation and characterizations

In a typical synthesis process, 0.05 M glucose and a controlled amount of PMMA were completely dissolved in 20 mL DMF solvent to form a homogeneous solution. The solution was then transferred into a Teflon-lined stainless steel autoclave (25 mL) and maintained at 160 °C for 3 h, and cooled naturally to room temperature. After the thermal treatment, the solution at the amount of 53 μL cm^{-2} was cast onto β″-alumina disks. The cast disks were dried overnight and finally calcined at 550 °C for 2 h under N_2 atmosphere. In order to realize different pore morphologies and thicknesses of the carbon films, different PMMA contents as listed in Table 1 were adopted for the casting. The porous carbon films on the β″-alumina substrate were directly characterized by X-ray diffraction (XRD) (Rigaku Ultima IV, Cu Kα radiation, λ = 1.5418 Å), scanning electron microscopy (SEM) (Hitachi S-3400N, 15.0 kV), and Raman spectroscopy (Witech CRM200, 532 nm). Fourier transform infrared (FTIR) spectra were recorded on a Bruker Tensor 27 operating in transmittance mode at normal incidence, using a spectral resolution of 4 cm^{-1}.

Table 1
Experimental parameters of the PCF samples.

Sample No.	Glucose concentration (M)	Amount of PMMA (g)	PMMA concentration (M)
PCF-1	0.05	0.2	0.1
PCF-2	0.05	0.3	0.15
PCF-3	0.05	0.4	0.2
PCF-4	0.05	0.6	0.3

2.3. Wettability test and electrochemical measurements

The wettability examination was carried on Krüss EasyDrop at 300 °C in an argon-filled glove box for 10 min (Mikrouna Universal

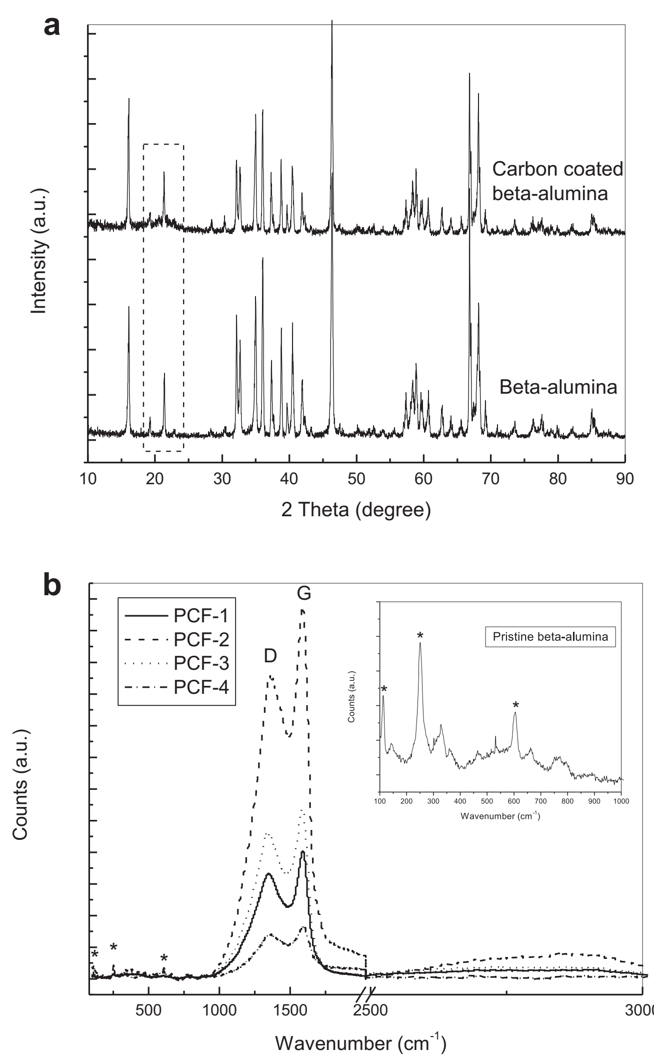

Fig. 1. (a) XRD patterns of β″-alumina ceramics with and without porous carbon coating. (b) Raman spectra of different porous carbon films coated β″-alumina ceramics. Inset is the Raman spectrum of pristine β″-alumina.

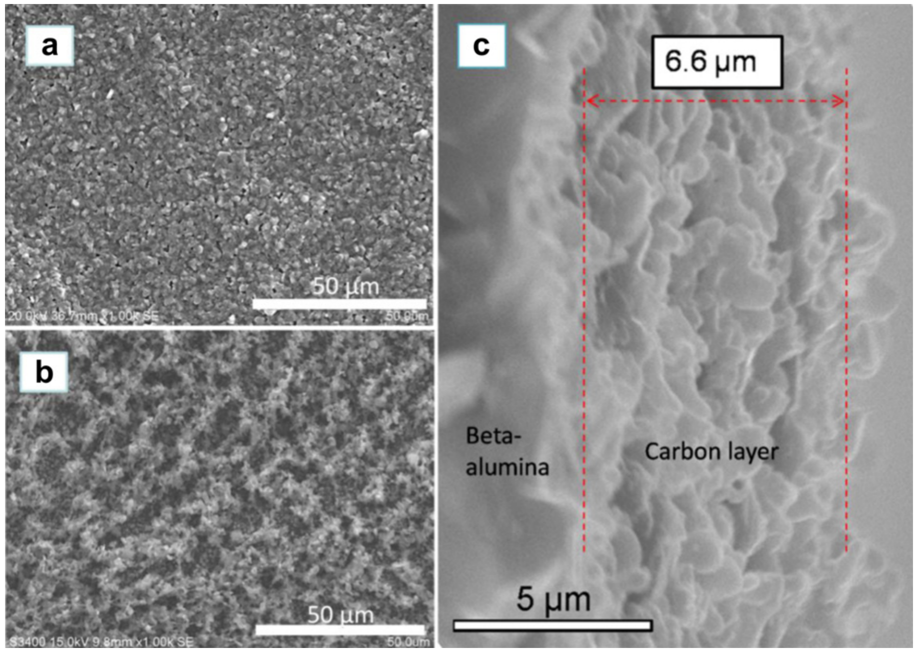

Fig. 2. SEM images of the surface of (a) pristine β″-alumina and (b) the typical PCF coated ceramics, and (c) a typical cross-section image of the PCF.

(2440/1000)) with oxygen and water contents lower than 1 ppm. All the samples were photographed and the contact angle was determined by a computer-supported tester. Electrochemical measurements were carried out using symmetric sodium electrode cells with β″-alumina ceramics with and without PCF modification as the electrolyte. The cell assembly was performed under vacuum environment. The cyclic voltammograms (CVs) were measured at 350 °C at the scan rate of 1 mV s^{-1}. Electrochemical impedance spectroscopy (EIS) measurements were conducted using a frequency response analyzer (Autolab PGSTAT302N) with an electrochemical interface (Autolab 4.9) in the frequency range from 1 MHz to 0.01 Hz.

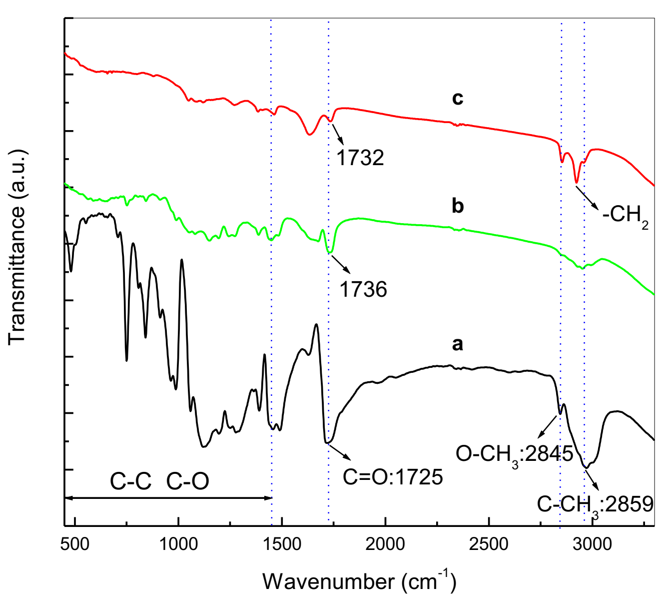

Fig. 3. FTIR spectra of (a) the precursor PMMA, the cast glucose-PMMA films by using a self-assembly solution (b) with and (c) without heat treatment at 160 °C for 3 h.

3. Results and discussion

3.1. Characterization of porous carbon films on β″-alumina surfaces

Fig. 1a shows the XRD pattern of a typical PCF prepared with 0.15 M PMMA on β″-alumina surface in comparison with that of the pristine β″-alumina ceramics. As indexed, all the distinct reflections correspond to the rhombohedral β″-alumina, while the broad band at around 21.5° would be considered to be corresponding to carbon (Joint Committee on Powder Diffraction Standards File Card No. 46-0945), indicating the formation of porous carbon film with low degree of crystallization. Fig. 1b displays the Raman spectra of the PCF samples as indicated in Table 1. As seen, all the coatings on β″-alumina exhibit D-band (the activated A_{1g} mode of the finite crystal size) at 1350 cm^{-1} and G-band (the E_{2g} mode of single crystal graphite) at 1580 cm^{-1}, manifesting the well-defined carbon coating layers [25,26]. Because the relative intensities of the D- and the G-band decrease with the increased degree of graphitization, the relatively high intensity of G-band suggests favorable graphitic level of these carbon coatings [22,25]. Moreover, the weak peaks from 100 cm^{-1} to 1000 cm^{-1} correspond to the β″-alumina substrate as confirmed by the image shown in the inset of Fig. 1b.

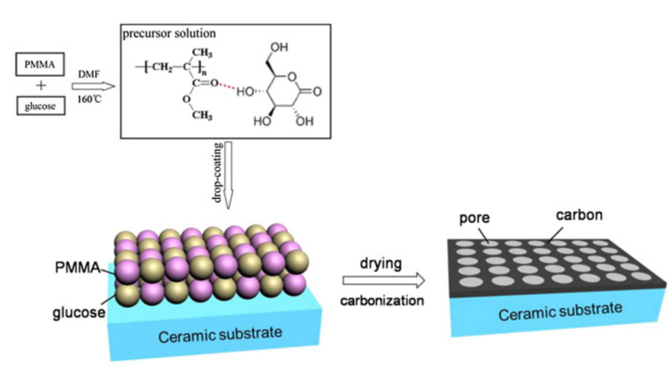

Fig. 4. Schematic illustration of the formation process of the typical PCF.

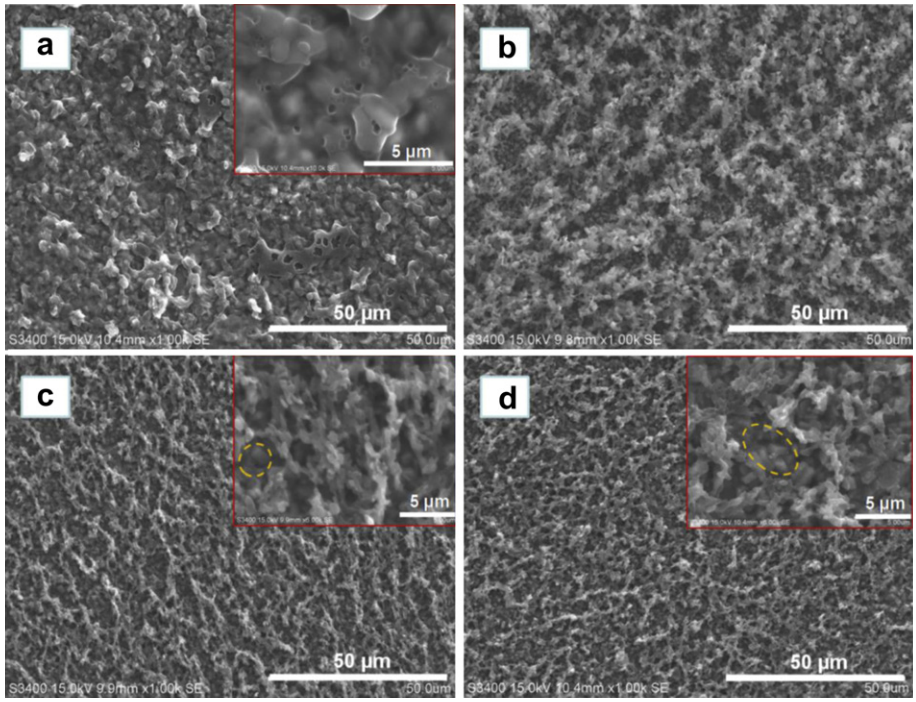

Fig. 5. SEM images of various porous carbon film coated β″-alumina ceramics: (a) PCF-1, (b) PCF-2, (c) PCF-3, and (d) PCF-4. Insets are the high-magnification images. The dashed circles indicate the uncoated β″-alumina ceramic substrates.

Fig. 2 illustrates the SEM images of the pristine β″-alumina ceramic surface and a typical PCF coating. As shown, the carbon film with micro-sized particles and uniformly distributed pores is obtained. The average pore size is approximately 5 μm. The cross-section image of the PCF is shown in Fig. 2c. A thickness of the carbon layer about 6.6 μm is displayed.

3.2. Formation mechanism and shape control of porous carbon films

PMMA has been commonly used as a pore-forming agent, because it could be easily wiped out during the sintering process [27,28]. However, it was usually considered as a hard template to attain porous materials, resulting in the nonuniformity of products through simple solid-phase mixing of source materials. In this work, a molecular-level connection between the carbon source (glucose) and pore-forming agent (PMMA) is realized in DMF solvent, which is crucial to ensure good dispersion of PMMA and to obtain a uniform porous carbon film finally. FTIR spectra of pure PMMA, and the cast hybrid glucose-PMMA films with and without heat treatment at 160 °C for 3 h are shown in Fig. 3. The characteristic peaks of PMMA at 1725 cm^{-1} (ester carbonyl stretch vibrations of C=O bonds), 2845 cm^{-1} ($O-CH_3$ vibrations), 2859 cm^{-1} ($C-CH_3$ vibrations), and the region lower than 1500 cm^{-1} (stretching and bending vibrations of C–C and C–O bonds) are observed [29,30]. It is seen that the addition of glucose shifts the peak at 1725 cm^{-1} remarkably to the higher energy side (1732 cm^{-1} and 1736 cm^{-1}), at the same time, weakens the C–C and C–O bonds. The mentioned vibrational frequency shift and weakened peaks are supposed to form the hydrogen bonds between the hydroxyl groups of glucose and the carbonyl oxygens of PMMA, which was also proved in other carbon precursors and polymer systems [21,23]. It is found that the heat treatment to some extent promotes the formation of the hydrogen bonds, leading to further shift of the peaks and even the disappearance of the peaks of $-CH_3$ bonds.

Fig. 4 schematically illustrates the hydrogen bonding between glucose and PMMA and the formation of porous carbon films on the basis of the above analysis. According to this proposed mechanism, we could modify the architecture of the PCFs by tuning the concentration of PMMA. Fig. 5 displays the SEM images of all the four PCFs obtained with different PMMA concentrations. As shown in Fig. 5a, the PCF-1 film from the solution of 0.1 M PMMA is very dense with a few pores of less than 1 μm in diameter. As the amount of PMMA increases, the porosity and pore size of the PCFs increase. It is obvious that a great part of the surface of the β″-alumina substrate is uncovered by PCF-3 and PCF-4 films, as shown in Fig. 5c and d. Furthermore, the thickness of the PCFs is also tested by SEM. The results are shown in Fig. 6. The PCF-2 film is more than three

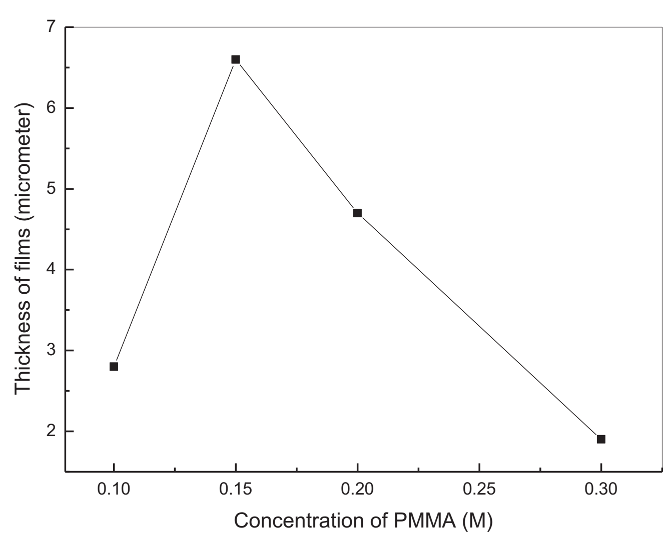

Fig. 6. Thickness of the PCFs prepared on the β″-alumina substrates.

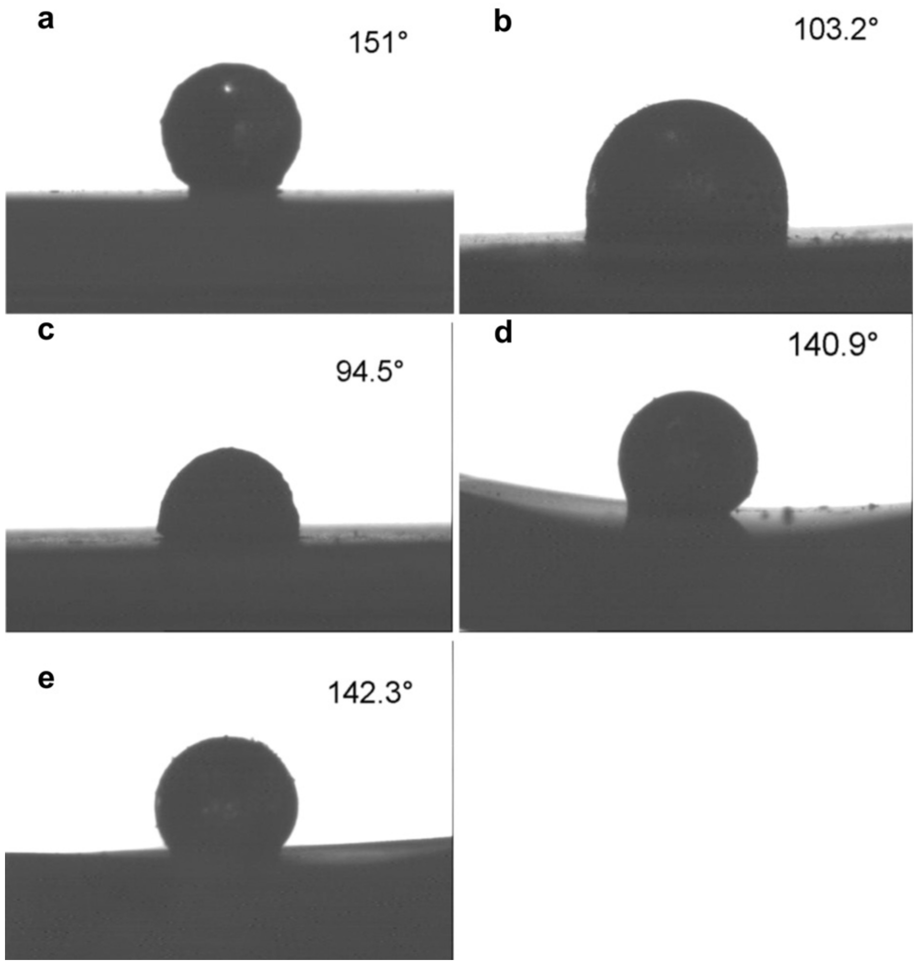

Fig. 7. Optical micrographs of the static sodium drop on (a) pristine β″-alumina, (b) PCF-1, (c) PCF-2, (d) PCF-3 and (e) PCF-4.

times thicker than the PCF-4. It is indicated that the porosity and thickness of PCFs to a great extent depend on the concentration of PMMA. As proposed in Fig. 4, the pores are formed owing to the evaporation of PMMA during annealing, the porosity of the PCFs thus increases with the increase of PMMA. It is found that the thickness of PCFs also correlated to the concentration of PMMA content in the precursor solution, and the largest thickness reached at the concentration of 0.15 M. As seen, the density of PCF-1 is very high, leading to a small thickness of the film. The film obtained from

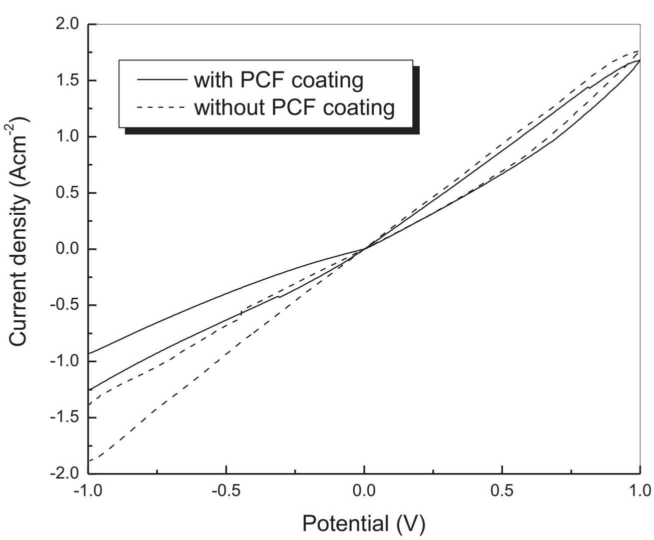

Fig. 8. Cyclic voltammetry of Na/β″-alumina/Na cell with and without the PCF coating at a scanning rate of 1 mV s^{-1} in the voltage window of −1.0 to 1.0 V.

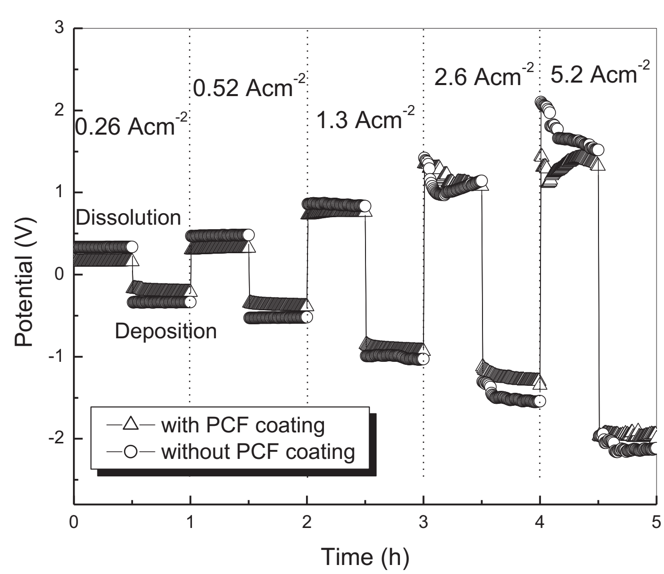

Fig. 9. Constant current polarization curves of Na/β″-alumina/Na cell with and without the PCF coating at 350 °C.

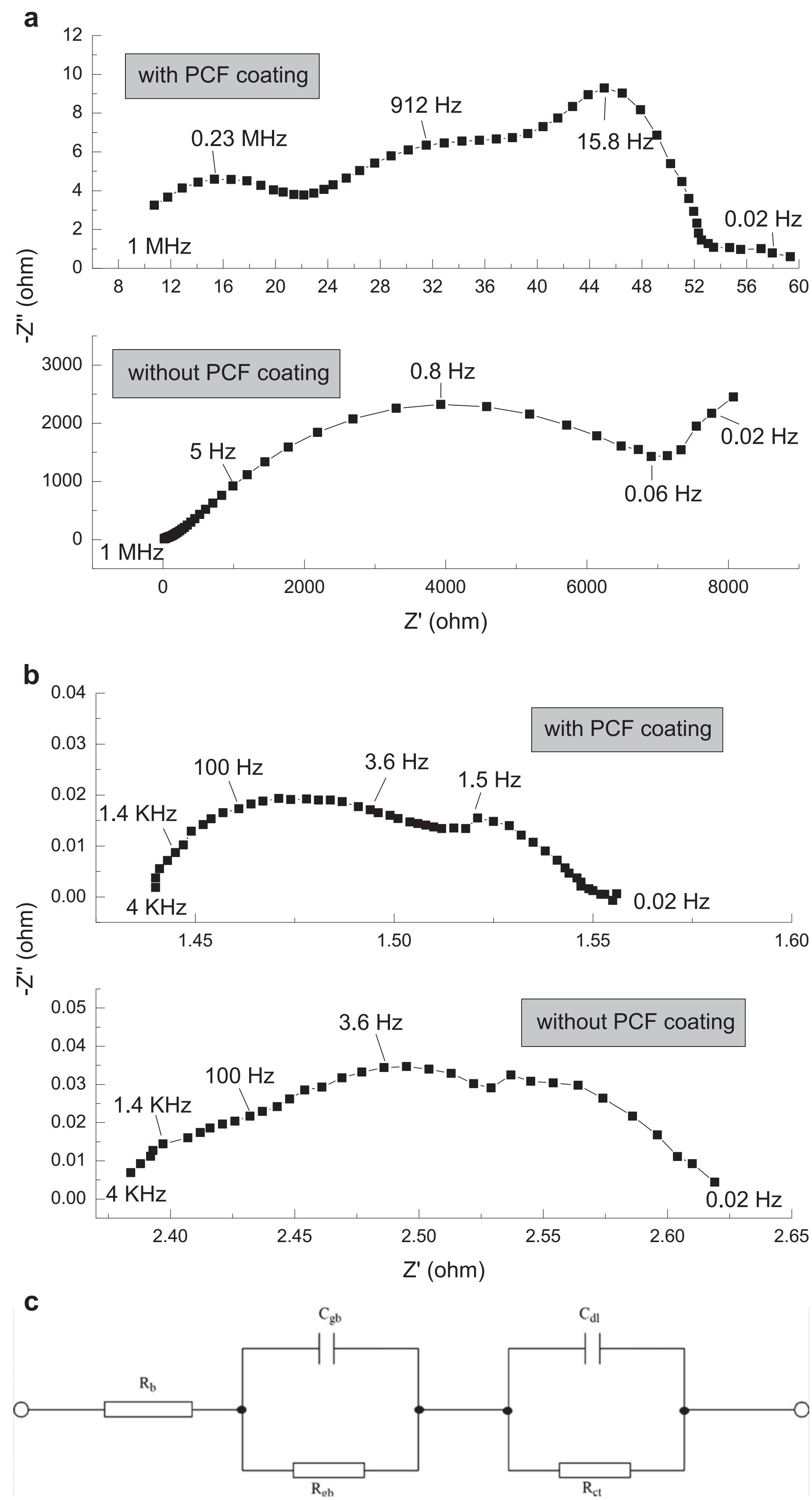

Fig. 10. Impedance spectra of Na/β″-alumina/Na with and without the PCF coating at 220 °C during the (a) heating and (b) cooling processes. (c) Corresponding fitted equivalent electrical circuit.

0.15 M PMMA solution contains much more pores, resulting in a lower density and the largest film thickness. The further increase in the PMMA concentration leads to thinner PCFs due to the lack of carbon sources.

Since the method has no special requirements for the substrate, it seems that this process to prepare carbon film can be applied to other compact ceramics besides the β″-alumina.

3.3. Wettability of the PCFs coated β″-alumina surface by sodium

The equilibrium contact angle was observed in 10 min at 300 °C, a temperature far above the melting point of sodium and close to the working temperature of Na-based batteries. The images of liquid sodium on the pristine and PCF modified β″-alumina ceramics were recorded by the contact angle analyzer and are shown in Fig. 7. As seen, the pristine β″-alumina represents almost non-wetting condition for molten sodium, in accordance with the previous reports [31]. While, as shown in Fig. 7b and c, the sodium droplets on the PCF-1 and PCF-2 modified β″-alumina ceramics become nearly hemispheres, with contact angles of 103.2° and 94.5°, respectively. Hence, the modification of the surface by PCF coating remarkably improves its wettability by molten sodium. It is noticed that the highly porous PCF-3 and PCF-4 modified β″-alumina ceramics illustrate only slightly improved wettability as shown in Fig. 7d and e. It is reasonable to propose that the wetting behavior is mainly determined by the porosity and density of the PCF coatings. The density of PCFs should be as large as possible, because sodium can reach more carbon soon after it becomes a liquid without affecting the transport of sodium ions. It can be seen that the wettability of the PCFs by sodium is improved as the density increasing. Furthermore, PCF-1 with higher density shows larger contact angle than PCF-2. It is thus speculated that the thickness of PCFs involving the substrate is another minor factor. The thickness should be large enough to satisfy the infiltration and diffusion of sodium on it rather than excessive contact with the non-wettable ceramics. As a result, the PCF-2 with favorable density and thickness has the best wettability by sodium.

3.4. Interfacial and polarization properties of the Na/β″-alumina/Na cells with and without the PCF coating

As demonstrated in the previous work [32,33], the considerable polarization could appear under certain conditions at the sodium/β″-alumina interface in the Na-based cells, because the molten sodium cannot be kept in contact with the whole operating area of the β″-alumina. According to our foregoing results, the PCF-2 can greatly improve the wettability of the β″-alumina surface for sodium. In order to identify the effect of the PCF coating on the interfacial and polarization properties of the sodium/β″-alumina system, Na/β″-alumina/Na symmetric cells with and without the PCF coating (PCF-2) were assembled through glass sealing. Cyclic voltammogram (CV) tests of the two cells at 350 °C were carried out at a scanning rate of 1 mV s^{-1} in the voltage window of −1.0 to 1.0 V (Fig. 8). CV curves of the two cells exhibit no redox peaks and asymmetric behavior, and the current density values for a given potential are smaller during the sodium dissolution than the sodium deposition, in accordance with the previous observation [34]. However, as can be seen, the hysteresis becomes smaller for the cell with the PCF coating. The polarization potentials of the Na/β″-alumina/Na cells with and without the PCF coating were measured as a function of the current density in Fig. 9. It can be seen that at low current densities (less than 0.52 A cm^{-2}), both cells reveal no obvious polarization, whereas at high current densities (higher than 1.3 A cm^{-2}), the polarization potential of the cell without coating becomes unstable with time, while the cell with coating shows stable polarization potential and better polarization performance. On the other hand, in order to demonstrate the improvement through the interfacial resistance, the impedance responses for the Na/β″-alumina/Na cells with and without the PCF coating at 220 °C during the heating and cooling processes are shown in Fig. 10. These impedance spectra show an intercept R_b on the real axis, corresponding to the bulk resistance of the β″-alumina, a semi-circle in the high frequency range derived from the grain boundary resistance of the β″-alumina electrolyte and a semi-circle at lower frequencies generated by the interfacial resistance. As previously reported [35], the interfacial resistance between molten sodium electrode and β″-alumina electrolyte was mainly charge-transfer resistance (R_{ct}) of Na^+ transport. As seen in Fig. 10(a) measured in the heating process, the interfacial resistance of the cell without coating is much larger than that with coating, which can explain that the β″-alumina with coating is wetted by sodium at a relatively low temperature (220 °C) instead of the pristine one. The fitting impedance values of the cells at 220 °C during the cooling process are shown in Table 2. When the temperature decreases to 220 °C, the interfacial resistance of the cell without coating increases to 0.12 Ω, twice of that with coating, and the C_{dl} values are similar. These results indicate that the Na/β″-alumina interface with carbon coating keeps its lower interfacial resistance during the cooling, ascribed to the remained favorable wetting behavior. Our work offers a solution to solve the polarization problem at the sodium/β″-alumina interface in the application of Na-based batteries.

Table 2
Impendence values of the Na/β″-alumina/Na cells with and without PCF coating at 220 °C during the cooling process.

Na/β″-alumina/Na cell	R_b (Ω)	R_{gb} (Ω)	C_{gb} (F)	R_{ct} (Ω)	C_{dl} (F)
Without PCF coating	2.37	0.048	9.5e−2	0.12	0.8
With PCF coating	1.438	0.021	0.06	0.055	0.17

4. Conclusion

In this paper, porous carbon films were successfully coated on the surface of the β″-alumina electrolyte through a low-cost and soft-template method. It is proposed that the effective connection between the carbohydrate and PMMA through hydrogen bonds promotes the uniformity of the porous carbon. The morphology and thickness of the synthesized PCFs can be controlled simply by varying the use-level of PMMA. This method is thought to be extended to any other compact ceramic surface. The coating greatly improves the wettability of the β″-alumina ceramic surface for sodium. The wetting behavior depends crucially on the thickness and porosity of the carbon coating. Moreover, the results of Na/β″-alumina/Na cells at 350 °C reveal that the polarization behavior of the cell is alleviated by the addition of the porous carbon coating. We anticipate that porous carbon films directly coated on the surface of the beta-alumina electrolyte may present a potential solution for the polarization problems at the sodium/beta-alumina interface in Na-based batteries.

Acknowledgments

The authors appreciate the financial support from the National Natural Science Foundation of China (No. 50730001), the Science and Technology Commission of Shanghai Municipality (No. 08DZ2210900), and Chinese Science and Technology Ministry (No. 2007CB209700). The help rendered by Dr. Jiadi Cao and Ms.

Yan Lu in constructing the sodium batteries and making a drawing is highly acknowledged.

References

[1] R. Walawalkar, J. Apt, R. Mancini, Energy Policy 35 (2007) 2558–2568.
[2] B. Dunn, H. Kamath, J.-M. Tarascon, Science 334 (2011) 928–935.
[3] F. Cheng, J. Liang, Z. Tao, J. Chen, Adv. Mater. 23 (2011) 1695–1715.
[4] J.L. Sudworth, J. Power Sources 100 (2001) 149–163.
[5] X. Lu, G. Xia, J.P. Lemmon, Z. Yang, J. Power Sources 195 (2010) 2431–2442.
[6] J.L. Sudworth, A.R. Tilley, The Sodium Sulphur Battery, Chapman & Hall, London, 1985.
[7] A.C. Buechele, L.C. De Jonghe, Am. Ceram. Soc. Bull. 58 (1979) 861.
[8] A. Imai, M. Harata, Jpn. J. Appl. Phys. 11 (1972) 180–185.
[9] I. Yasui, R.H. Doremus, J. Electrochem. Soc. 125 (1978) 1007–1010.
[10] C.C. Addison, E. Iberson, J. Chem. Soc. (1965) 1437.
[11] C.C. Addison, E. Iberson, R.J. Pulham, Soc. Chem. Indust. Monograph 28 (1968) 246.
[12] R. Knoedler, W. Baukal, W.H. Kuhn, J. Electrochem. Soc. 124 (1977) 236–237.
[13] M.L. Wright, UK Patent Application 2067005 (1981).
[14] A.G. Montgomery, UK Patent 1530274 (1978).
[15] A.R. Tilley, M.D. Hames, J.L. Sudworth, J.M. Bird, UK Patent 1511152 (1978).
[16] A.I. Belyaev, D.B. Butrymowicz, Surface Phenomena in Metallurgical Process, Consultants Bureau Enterprises Inc., New York, 1965.
[17] R. Ryoo, S.H. Joo, S. Jun, J. Phys. Chem. B 103 (1999) 7743–7746.
[18] B. Sakintuna, Y. Yurum, Ind. Eng. Chem. Res. 44 (2005) 2893–2902.
[19] J. Kim, J. Lee, T. Hyeon, Carbon 42 (2004) 2711–2719.
[20] D. Kawashima, T. Aihara, Y. Kobayashi, T. Kyotani, A. Tomita, Chem. Mater. 12 (2000) 3397–3401.
[21] C. Liang, K. Hong, G.A. Guiochon, J.W. Mays, S. Dai, Angew. Chem. Int. Ed. 43 (2004) 5785–5789.
[22] G. Liu, Y. Liu, Z. Wang, X. Liao, S. Wu, W. Zhang, M. Jia, Micropor. Mesopor. Mater. 116 (2008) 439–444.
[23] A.T. Rodriguez, X. Li, W.A. Steen, H. Fan, Adv. Funct. Mater. 17 (2007) 2710–2716.
[24] Z. Wen, Z. Gu, X. Xu, J. Cao, F. Zhang, Z. Lin, J. Power Sources 184 (2008) 641–645.
[25] F. Tuinstra, J.L. Koenig, J. Chem. Phys. 53 (1970) 1126.
[26] E.H. Lee, D.M. Hembree Jr., G.R. Rao, L.K. Mansur, Phys. Rev. B 48 (1993) 15540.
[27] Y. Yu, L. Gu, C. Zhu, P.A. Aken, J. Maier, J. Am. Chem. Soc. 131 (2009) 15984–15985.
[28] M. Boaro, J.M. Vohs, R.J. Gorte, J. Am. Ceram. Soc. 86 (2003) 395–400.
[29] K. Moller, T. Bein, R.X. Fischer, Chem. Mater. 10 (1998) 1841–1852.
[30] B. Schneider, J. Stokr, P. Schmidt, M. Mihailov, S. Dirlikov, N. Peeva, Polymer 20 (1979) 705–712.
[31] C.J. Wung, Y. Pang, P.N. Prasad, F.E. Karasz, Polymer 32 (1991) 605–608.
[32] L. Viswanathan, A.V. Virkar, J. Mater. Sci. 17 (1982) 753–759.
[33] D.A. Bradhurst, A.S. Buchanan, Aust. J. Chem. 14 (1961) 397–408.
[34] L. Geneva, Fast Ion Transport in Solids, North-Holland, New York, 1973.
[35] R.D. Armstrong, T. Dickinson, J. Turner, Electroanal. Chem. Interfac. Electrochem. 44 (1973) 157–167.